# Supplemental Materials for

## Distinct antibody repertoires against endemic human coronaviruses in children and adults

Taushif Khan, Mahbuba Rahman, Fatima Al Ali, Susie S. Y. Huang, Manar Ata, Qian Zhang, Paul Bastard, Zhiyong Liu, Emmanuelle Jouanguy Vivien Béziat, Aurélie Cobat, Gheyath K. Nasrallah, Hadi M. Yassine, Maria K. Smatti, Amira Saeed, Isabelle Vandernoot, Jean-Christophe Goffard, Guillaume Smits, Isabelle Migeotte, Filomeen Haerynck, Isabelle Meyts, Laurent Abel, Jean-Laurent Casanova, Mohammad R. Hasan, Nico Marr*

JCI Insight (February 3, 2021) version

*Corresponding author: Nico Marr, Sidra Medicine, Research Branch, Al Gharrafa Street, Ar-Rayyan, PO BOX 26999, Doha, Qatar, E-mail: nmarr@sidra.org

**Content[#]**



[#]Supplemental Tables 3 and 4 are provided as spreadsheets in a separate file.

# Supplemental Figures

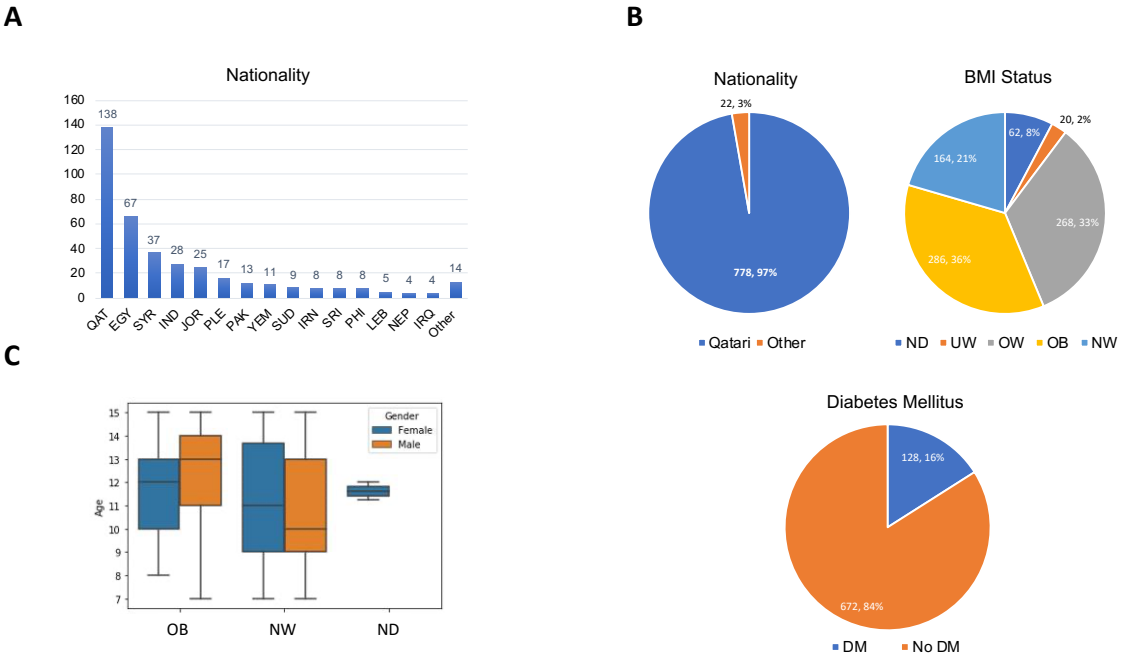


**Supplemental Figure 1. Demographic and clinical features of the different human cohorts. A,** Nationalities among the healthy blood bank donors. **B,** Number and fraction of Qatari nationals and long-term residents with other nationality comprising the 800 assayed individuals of the Qatar Biobank cohort, stratified by body mass index (BMI) and proportion of subjects with diabetes mellitus (DM). UW, underweight (BMI < 18); NW, normal weight (BMI ≥ 18 and < 25); OW, overweight (BMI ≥ 25 and <30); OB, obese (BMI ≥ 30). **C,** Number and fraction of male and female pediatric study subjects with normal weight (NW) or who were obese (OB). ND, not determined; QAR, Qatar; EGY, Egypt; SYR, Syria; IND, India; JOR, Jordan; PAK, Pakistan; YEM, Yemen; SUD, Sudan; IRN, Iran; SRI, Sri Lanka; PHI, Philippines; LEB, Lebanon; NEP, Nepal; IRQ, Iraq; Other, residents with other nationality; PLE, non-residents.

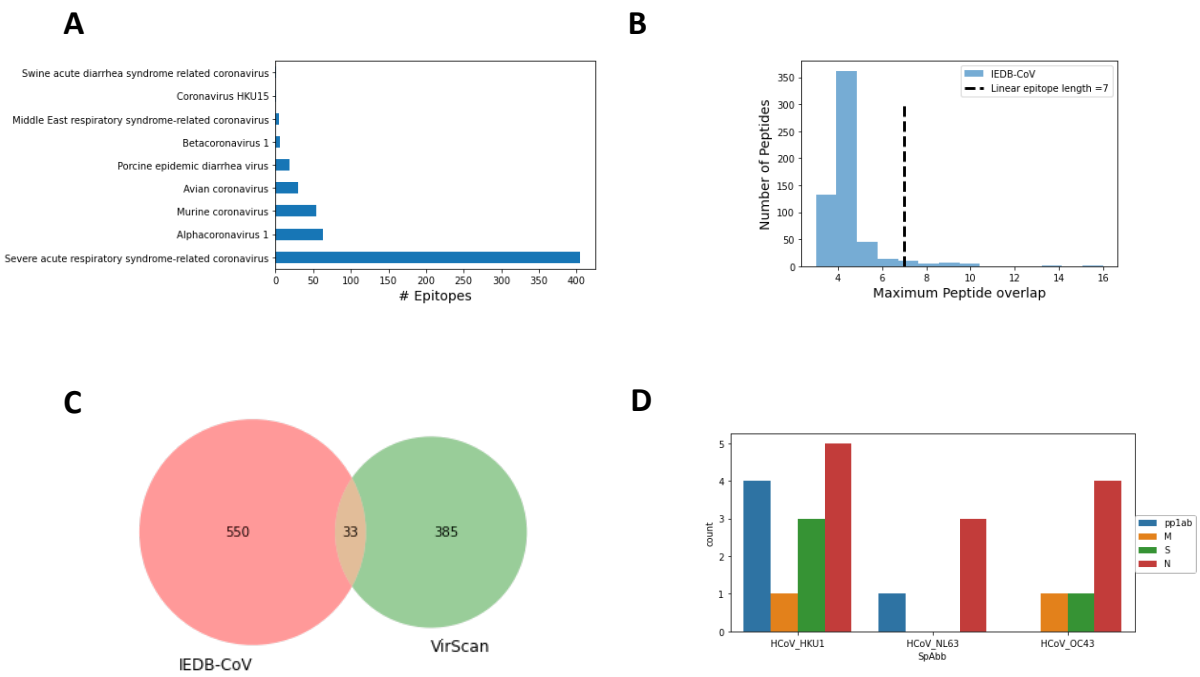


**Supplemental Figure 2. Comparison analysis of enriched HCoV peptides identified by PhIP-Seq with B cell epitopes in the Immune Epitope Database (IEDB). A**, Number of B cell epitopes for different CoV species available in IEDB (accessed and downloaded from www.iedb.org on 17 May 2020). **B**, Number of peptides from endemic HCoVs which we found to be significantly enriched in at least three of all samples (*N* = 1399) with homology in the linear amino acid sequence to 583 known CoV B cell epitopes in IEDB. We considered an epitope as a match if there was ≥ 7 linear sequence identity between query (IEDB epitope) and the amino acid sequence of the enriched HCoV peptide. **C,** Venn diagram depicting overlap between enriched peptides (i.e. matches) detected by VirScan and B cell epitopes from CoVs in IEDB. **D**, Number of matching peptides that share sequence homology with known B cell epitopes, stratified by species and viral protein.

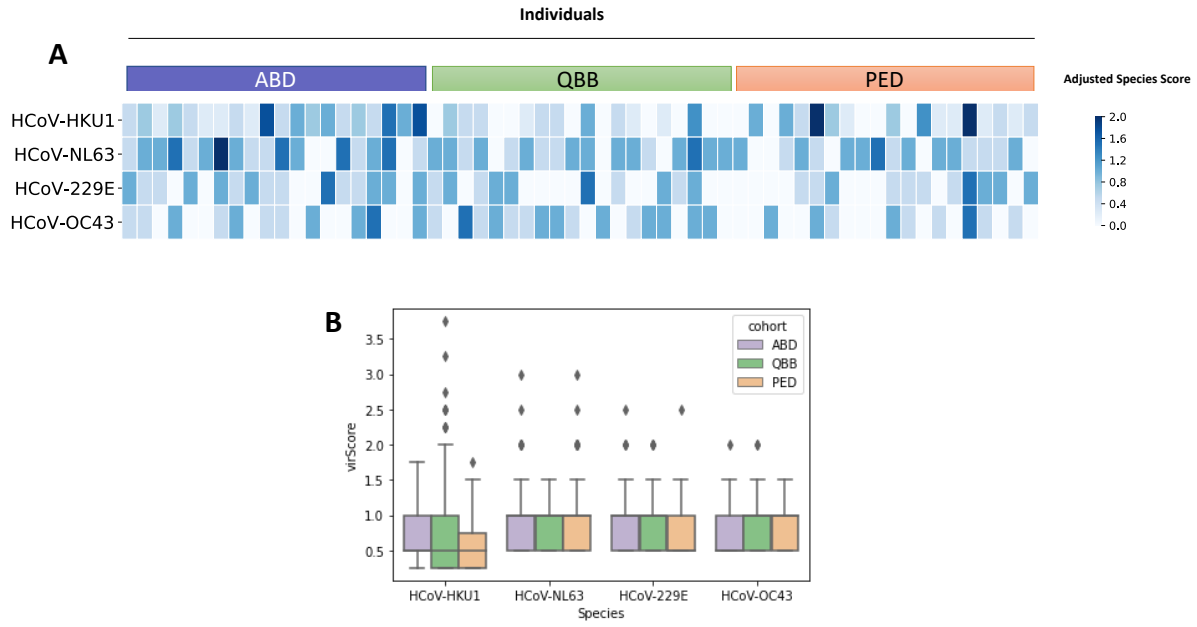


**Supplemental Figure 3: Similar antibody repertoire breadth among seropositive individuals of the different cohorts. A**, Heatmap plot depicting adjusted species score values for HCoV-HKU1, -NL63, -229E and -OC43 in randomly selected seropositive individuals (*n* = 20) of each cohort. Each individual is represented as a column. Values $\geq 1$ indicate that the individual was seropositive for a given species. **B**, Species-wise variation in adjusted species score values among seropositive individuals of each cohort.

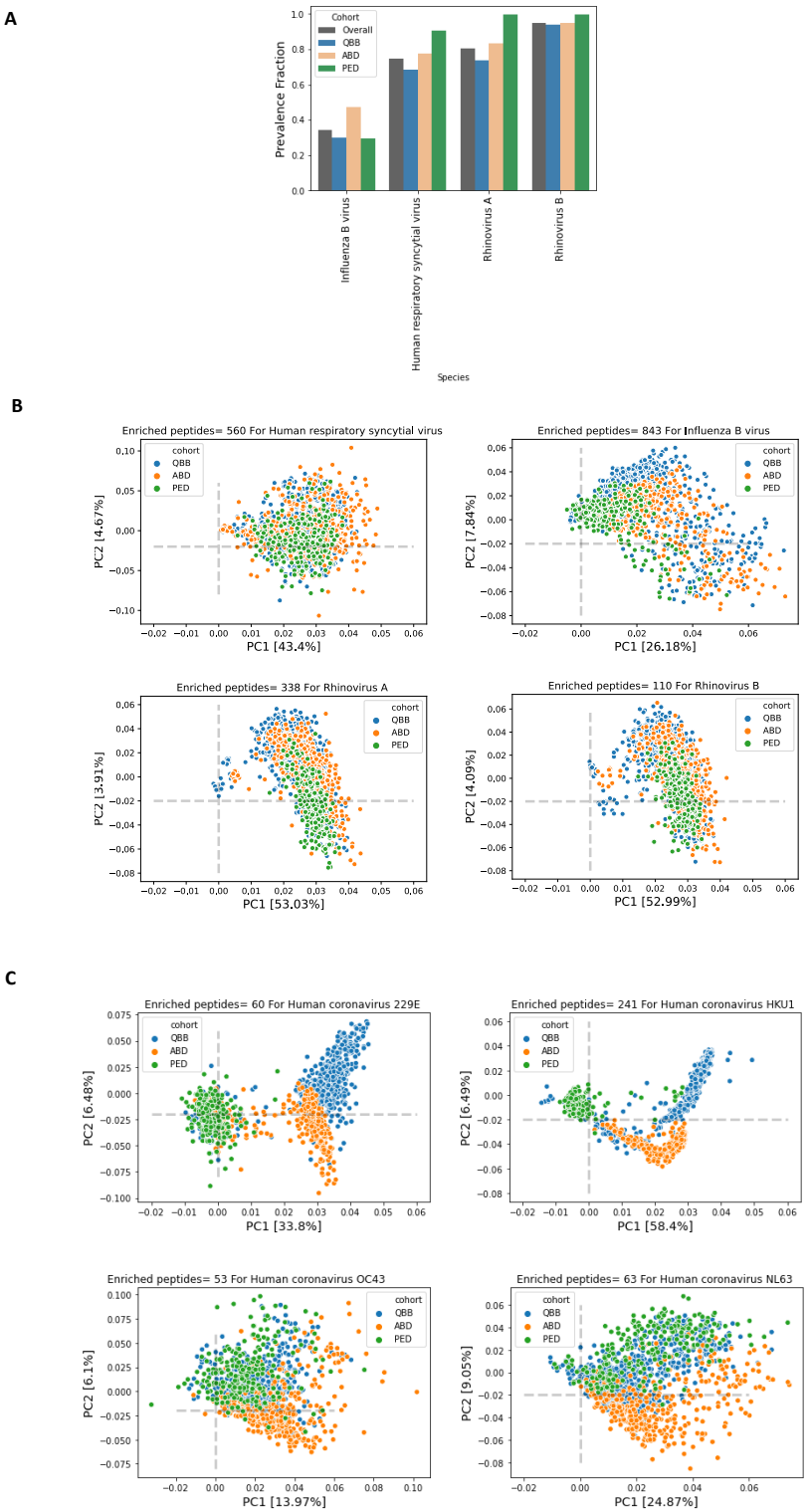


**Supplemental Figure 4. Seroprevalence of respiratory viruses and variance in the antibody repertoires among individuals of the analyzed cohorts. A,** Bar plot depicting the fraction of individuals found seropositive for human respiratory syncytial virus, rhinovirus A, rhinovirus B and influenza B virus among the tested subjects or by cohort. **B** and **C,** Principal component analysis of the antigenic peptides of human respiratory syncytial virus, rhinovirus A, rhinovirus B and influenza B virus **(B)**, as well as of human coronaviruses 229E, NL63, OC43 and HKU1 **(C)**, that we found to be enriched in at least 3 samples.

# Supplemental Figure 5A

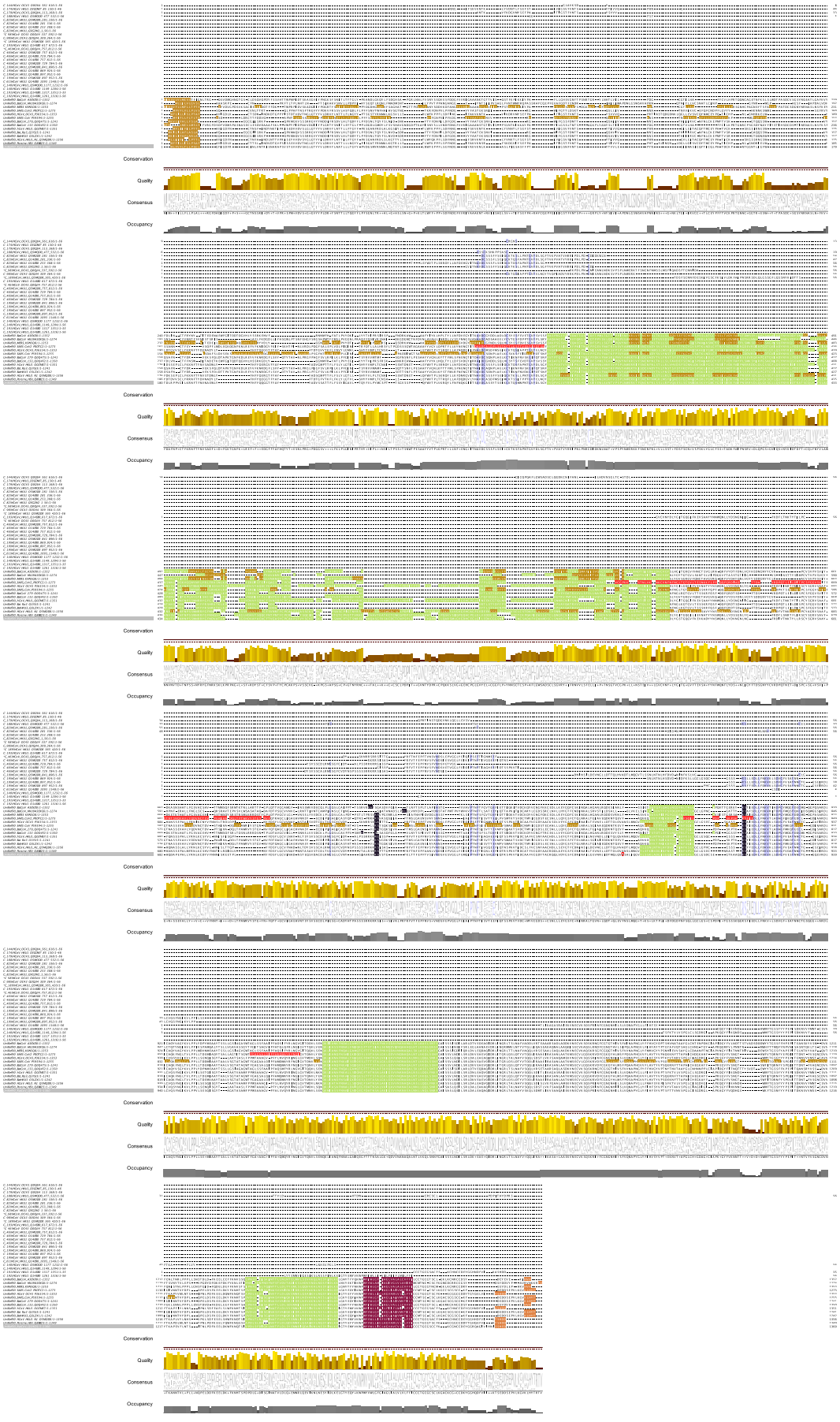

# Supplemental Figure 5B

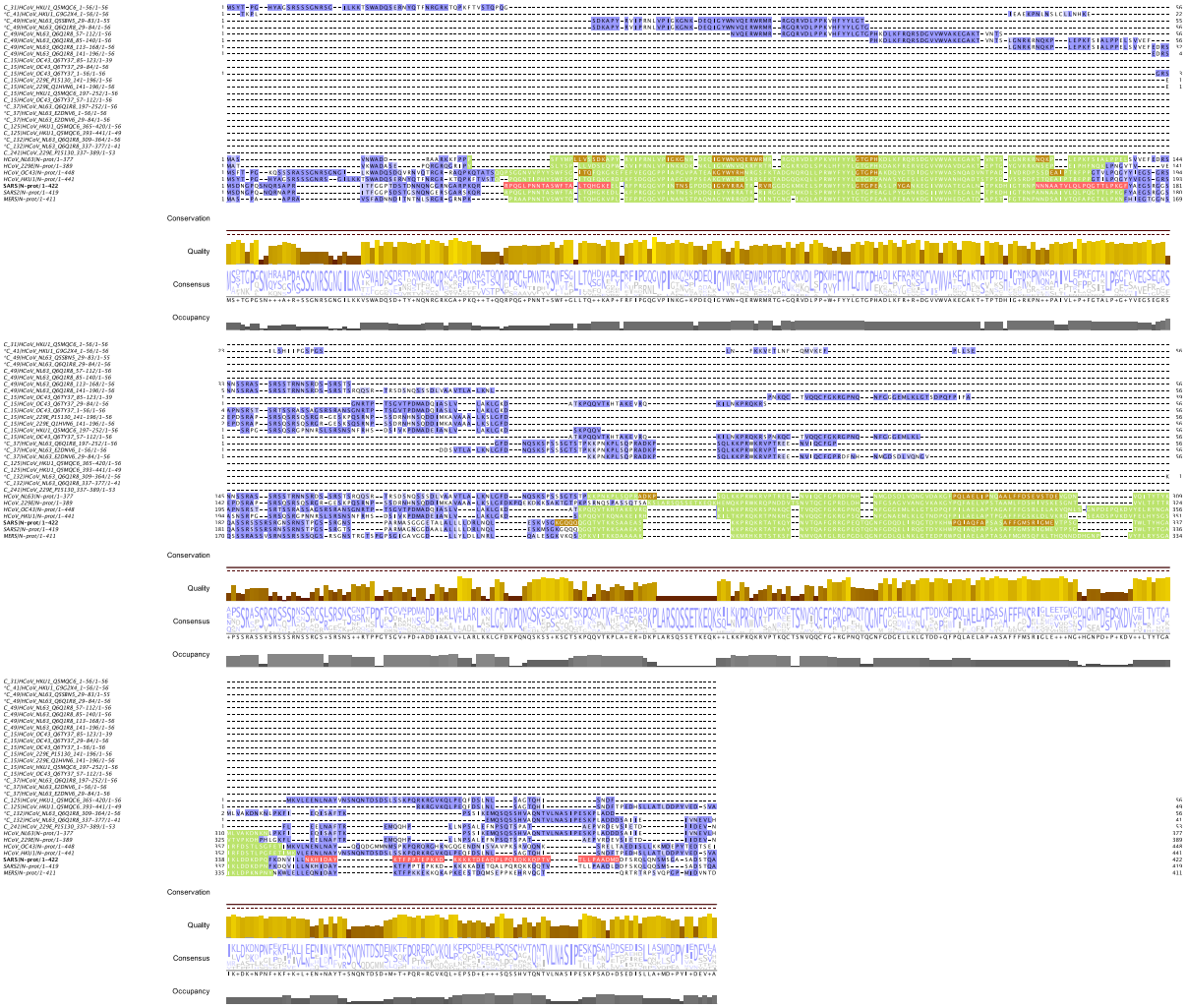

# Supplemental Figure 5C

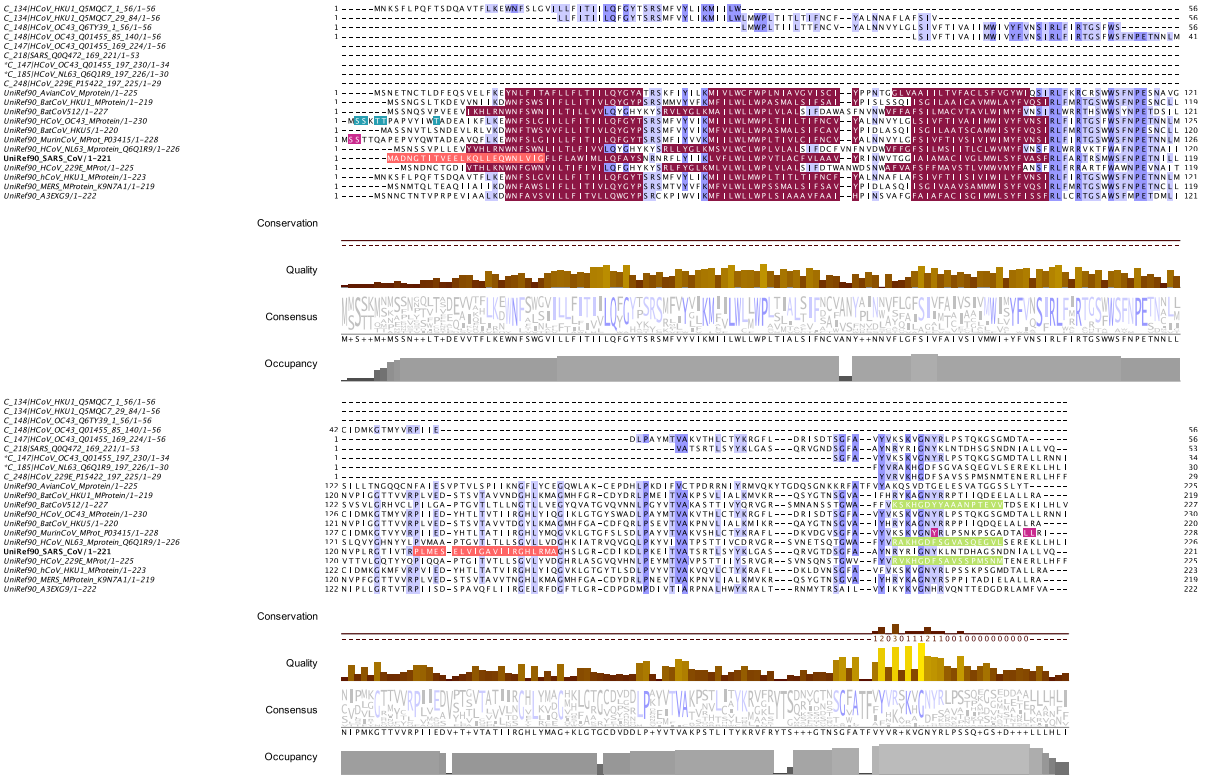

## Supplemental Figure 5D

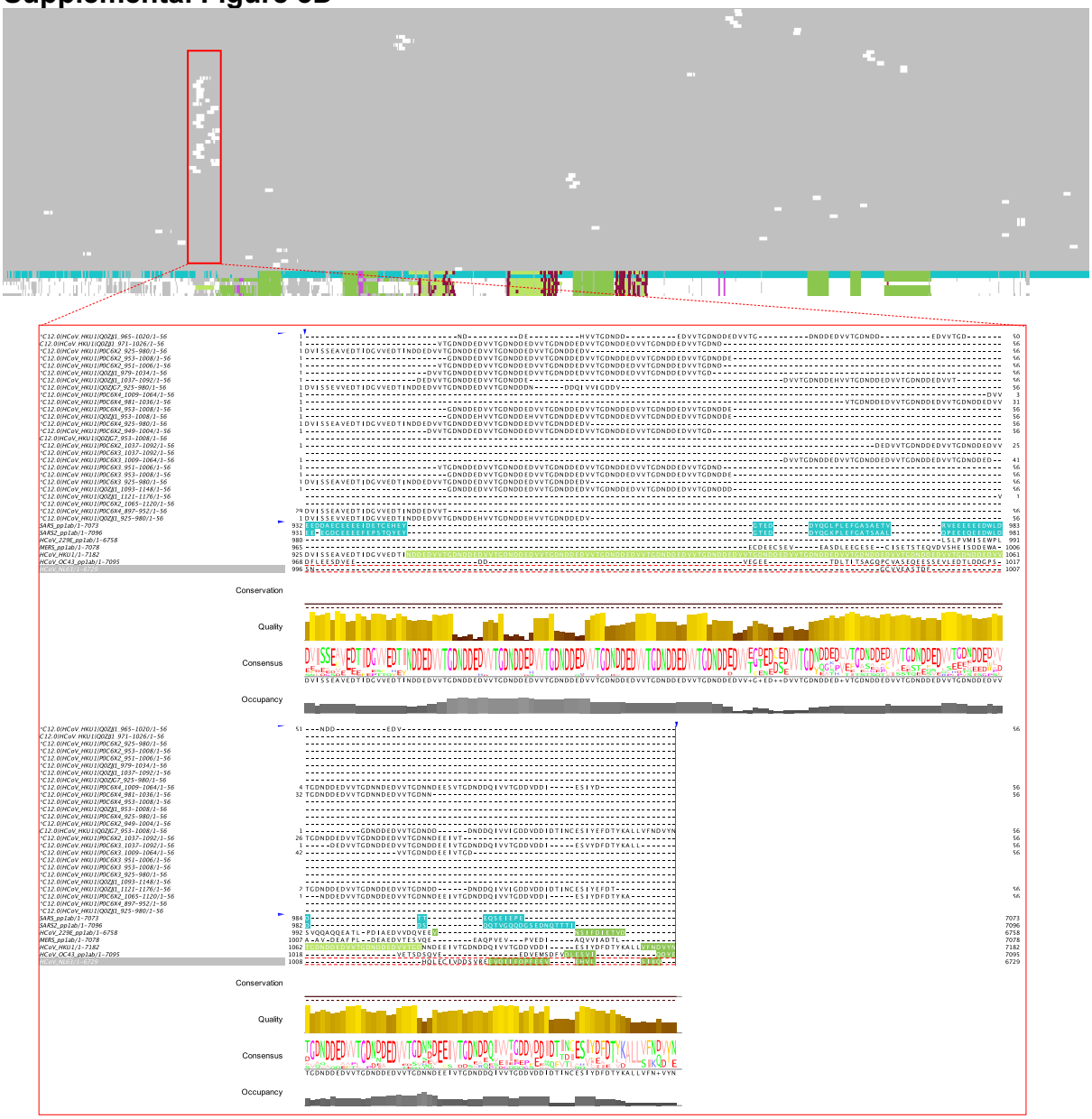


**Supplemental Figure 5. Mapping of enriched, immunodominant peptides of endemic HCoVs to the full-length protein sequences**. **A-D**, Multiple sequence alignments of the enriched, immunodominant peptides with the full-length sequences of the spike protein **(A)**, nucleocapsid protein **(B)**, matrix glycoprotein **(C)** and the Orf1ab replicase polyprotein **(D)** of selected coronaviruses. Amino acids with a high percentage of sequence identity are shown in violet. Reference sequence features are color-coded in accordance with the annotation and features available in UniProtKB and visualized using JalView. Green indicates regions of interest, red indicates transmembrane regions, orange indicates beta strands and pink indicates residues annotated as epitopes in IEDB. The cleavage sites (S1/S2 and S2') of the SARS-CoV S protein are shaded in black. For pp1ab, the sequence alignment is shown as an overview with gaps are shaded in grey and sequences are in white. Only part of the sequence alignment is shown, which depicts the PL1-PRO cleavage product containing a tandem repeat of N-[DN]-D-E-D-V-V-T-G-DA in HCoV-HKU1 (isolate N1) (UniProtKB entry and position P0C6X2[945-1084]).

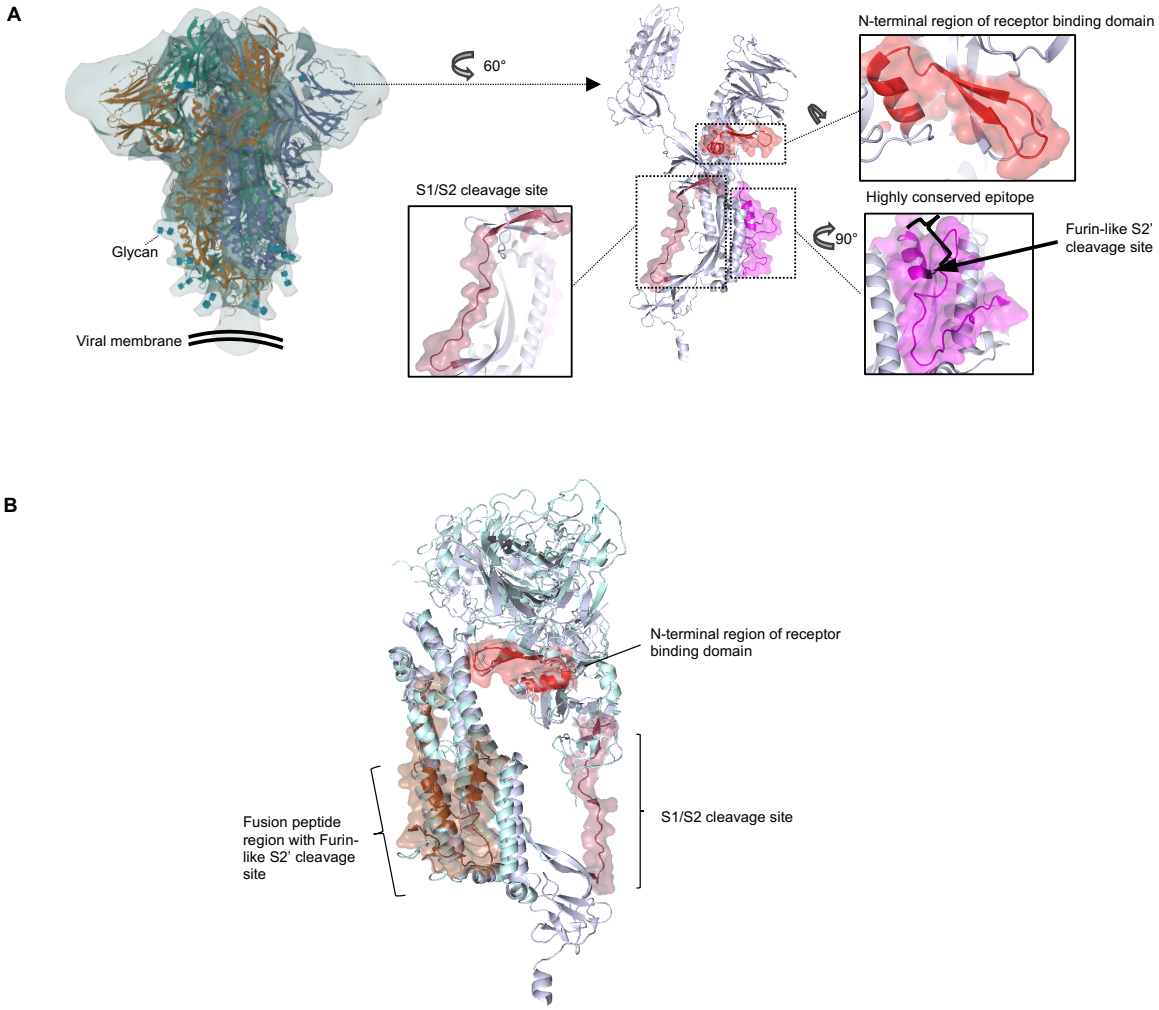


**Supplemental Figure 6. Antigenic regions of the spike protein. A,** Ribbon diagram of the SARS-CoV-2 S trimer with carbohydrate residues shown (left) and monomer without carbohydrate residues (middle) in the prefusion conformation (PDB id: 6VXX, chain A); regions for which multiple sequence alignments are shown in Figures 3C-E are depicted enlarged. **B,** Superimposition of the spike proteins of SARS-CoV-2 (6VXX) and HCoV-HKU1 (5I08) in the prefusion state. Root-mean-square deviation [rmsd] = 3.328 Ångström.

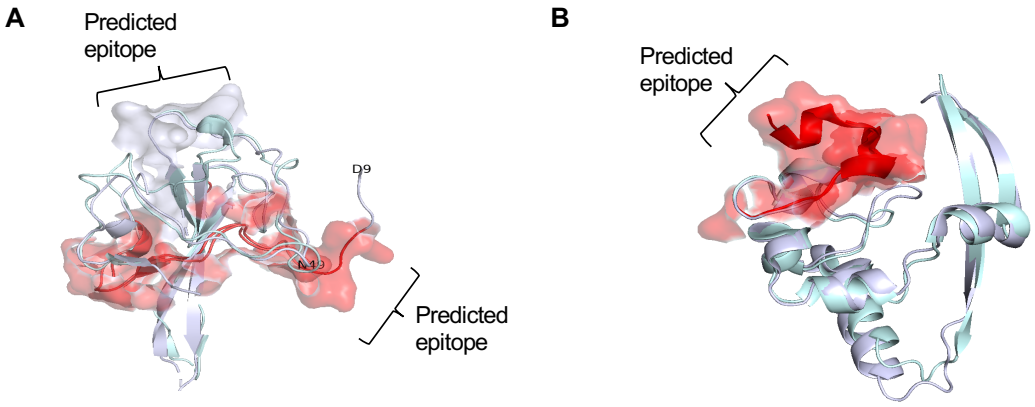


**Supplemental Figure 7. Structurally conserved immunodominant regions of the nucleocapsid protein. A,** Super-imposed ribbon structure of the N-terminal RNA-binding domain from HCoV-NL63 (PDB: 5N4k, chain A) and that from SARS-CoV-2 (PDB: 6M3M, chain A) (root-mean-square deviation [rmsd] = 0.7 Ångström). **B,** Super-imposed ribbon structure of the C-terminal self assembly domain of proteins from HCoV- NL63 (pdbId: 5EPW, chain A) and that of SARS-CoV-2 (pdbID: 6WJI, chain A) (rmsd = 0.91 Ångström).

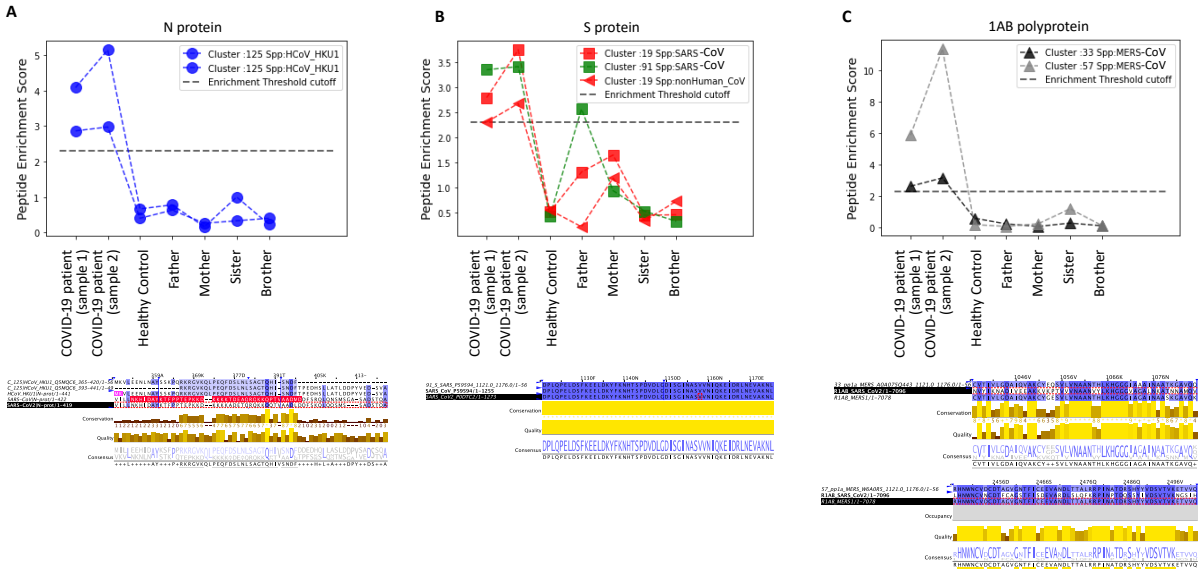


**Supplemental Figure 8. Cross-reactive antibody responses in a COVID-19 patient with proteins of other coronaviruses. A-C**, Plasma samples of an adult COVID-19 patient, unexposed family members (father, mother, sister and brother) as well as an unrelated healthy, age- and gender-matched control were subjected to PhIP-Seq analysis. Samples from the COVID-19 patient were obtained at two time points: during acute infection (sample 1) and during the convalescent phase, one week after hospital discharge (sample 2). Shown is a comparison of enrichment scores of peptides derived from the N protein **(A)**, S protein **(B)** and 1AB polyprotein **(C)** of various coronaviruses. HCoV-HKU1 peptides are depicted as circles, SARS-CoV peptides are depicted as squared symbols and MERS-CoV as well as non-human CoV peptides are shown as triangles. SARS-CoV-2 peptides were not included in the VirScan phage library used in our study. The dashed line indicates the significance cut-off for the peptide enrichment [$-\log10(P) \geq 2.3$]. The cluster numbers indicate linear epitopes as listed in Table S3. The multiple sequence alignments (bottom) of the enriched peptides with the reference sequences of SARS-CoV-2 and the respective CoV species show the degree of sequence identity across species. Known epitopes in the Immune Epitope Database (IEDB) are shown in pink. Sequences were colored to indicate percent sequence identity and visualized using Jalview.

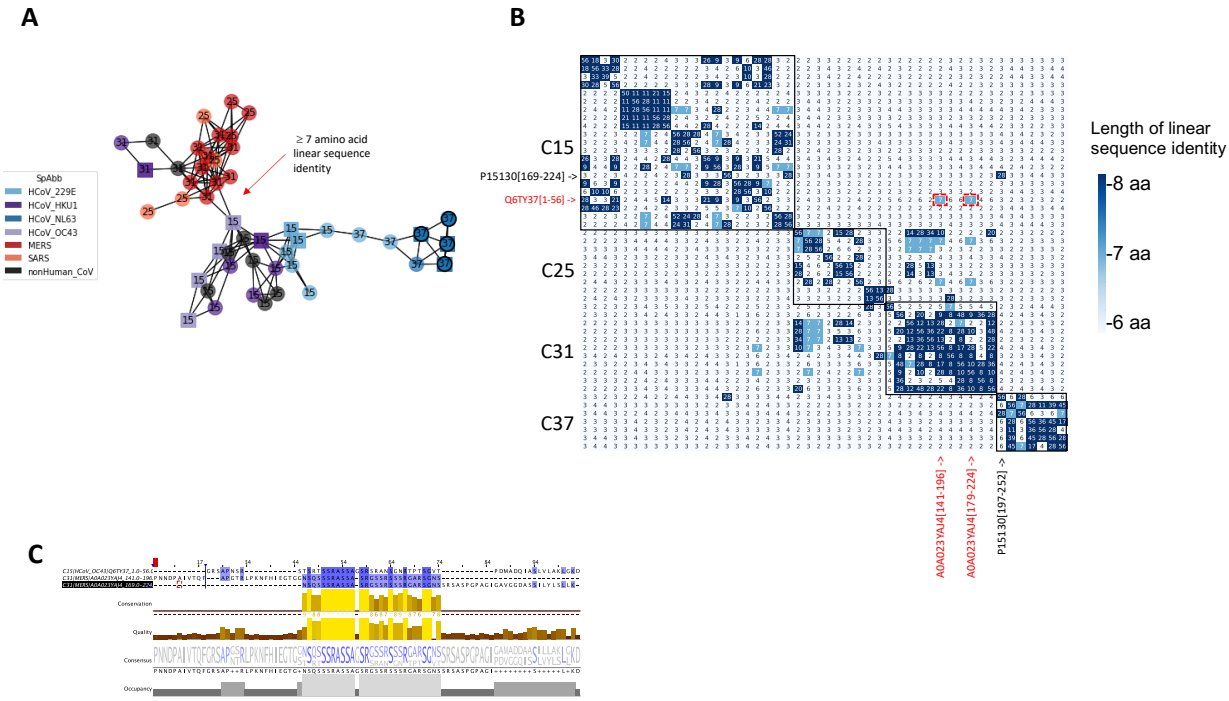


**Supplemental Figure 9. Clustering of peptides for shared linear B cell epitopes. A**, Network representation of peptides built from a pairwise distance matrix as shown in Figure 5B. Each node represents an enriched peptide and the color indicates the species. Edges indicate ≥ 7 amino acids linear sequence identity between two nodes (i.e. peptides), the estimated size of a linear B cell epitope. **B**, Pairwise distance matrix of peptides targeted by cross-reactive antibodies, including enriched peptides of clusters 15, 25, 31 and 37. The cluster assignment has been indicated as a black box. Distance pairs with ≥ 7 amino acid linear sequence identity are shown in dark blue. Distance pairs marked with a red box represent a 7 amino acid linear sequence identity between enriched peptides of more distantly related CoVs, namely HCoV-OC43 (Q6TY37[1-56]) and MERS-CoV (A0A023YAJ4[141-196] and A0A023YAJ4[179-224]). **C**, Multiple sequence alignment of enriched HCoV-OC43- and MERS-CoV-derived peptides Q6TY37[1-56], A0A023YAJ4[141-196] and A0A023YAJ4[179-224] encoding part of the N-terminal intrinsically disordered region (IDR) of the N protein. The alignment shows the 7 amino acid linear sequence identity in a low-complexity sequence motive (SSRASSA) which likely represents a broadly cross-reactive antibody binding site.

# Supplemental Tables

**Supplemental Table 1. Proteins of CoVs represented in the VirScan phage library**

| *Species*[A] | *Organism* | *Protein* | *No. of Peptides* |
|---|---|---|---|
| *Alphacoronavirus 1* | Feline coronavirus (strain FIPV WSU-79/1146) (FCoV) | NS | 239 |
| *Bat coronavirus 1B* | Bat coronavirus 1B | Rep1a | 249 |
| *Betacoronavirus 1* | Bovine coronavirus | N | 4 |
| | Bovine coronavirus (strain 98TXSF-110-ENT) (BCoV-ENT) (BCV) | E | 2 |
| | | N | 7 |
| | | NS | 12 |
| | | S | 48 |
| | Equine coronavirus | Rep1a | 254 |
| | **Human coronavirus OC43 (HCoV-OC43)** | **HE** | **15** |
| | | **M** | **11** |
| | | **N** | **4** |
| | | **NS** | **253** |
| | | **S** | **37** |
| | Porcine hemagglutinating encephalomyelitis virus (strain 67N) (HEV-67N) | N | 16 |
| ***Human coronavirus 229E*** | **Human coronavirus 229E (HCoV-229E)** | **E** | **2** |
| | | **M** | **8** |
| | | **N** | **23** |
| | | **NS** | **248** |
| | | **ORF4** | **10** |
| | | **Rep1b** | **2** |
| | | **S** | **63** |
| ***Human coronavirus HKU1*** | **Human coronavirus HKU1 (HCoV-HKU1)** | **N** | **13** |
| | | **Rep1ab** | **510** |
| | | **S** | **15** |
| | **Human coronavirus HKU1 (isolate N1) (HCoV-HKU1)** | **E** | **2** |
| | | **HE** | **13** |
| | | **M** | **7** |
| | | **N** | **22** |
| | | **NS** | **259** |
| | | **S** | **48** |
| | **Human coronavirus HKU1 (isolate N2) (HCoV-HKU1)** | **E** | **2** |
| | | **HE** | **13** |
| | | **N** | **7** |
| | | **NS** | **258** |
| | | **S** | **48** |
| | **Human coronavirus HKU1 (isolate N5) (HCoV-HKU1)** | **NS** | **254** |
| ***Human coronavirus NL63*** | **Human coronavirus NL63 (HCoV-NL63)** | **E** | **2** |
| | | **M** | **10** |
| | | **N** | **18** |
| | | **NS** | **248** |
| | | **ORF3** | **1** |
| | | **Rep1a** | **1** |
| | | **S** | **71** |
| ***Middle East respiratory syndrome coronavirus*** | BtVs-BetaCoV/SC2013 | E | 2 |
| | | M | 7 |
| | | N | 15 |
| | | ORF3 | 3 |
| | | ORF4 | 11 |
| | | ORF5 | 8 |
| | | ORF8 | 6 |
| | | Rep1a | 256 |
| | | S | 47 |
| | Coronavirus Neoromicia/PML-PHE1/RSA/2011 | E | 2 |
| | | ORF3 | 3 |
| | | ORF4 | 12 |
| | | ORF5 | 7 |
| | | ORF8 | 7 |
| | | Rep1a | 156 |
| | | S | 47 |
| | Human coronavirus EMC (isolate United Kingdom/H123990006/2012) (HCoV-EMC) | E | 2 |
| | | M | 7 |
| | | N | 14 |
| | | NS | 408 |
| | | ORF3 | 3 |
| | | ORF4 | 11 |
| | | ORF5 | 7 |
| | | S | 48 |
| | Middle East respiratory syndrome coronavirus | N | 8 |
| | | ORF4 | 11 |
| | | ORF5 | 11 |
| | | ORF8 | 3 |
| | | Rep1a | 1018 |
| | | Rep1ab | 95 |
| | | Rep1b | 63 |
| | | S | 108 |
| *Severe acute respiratory syndrome-related coronavirus* | Bat coronavirus 279/2005 (BtCoV) (BtCoV/279/2005) | E | 2 |
| | | M | 7 |
| | | NS | 254 |
| | | U | 2 |
| | Human SARS coronavirus (SARS-CoV) | N | 15 |
| | | NS | 9 |
| | | ORF3 | 9 |
| | | ORF7 | 4 |
| | | ORF9 | 3 |
| | | S | 44 |
| | Human SARS coronavirus (isolate Tor2) (SARS-CoV) | Rep1b | 1 |

[A]Proteins of endemic hCoVs are shown in bold.

**Supplemental Table 2. Number of individuals included in the downstream analysis**

| Cohort | Gender | No. of subjects | Age (years) | | | |
|---|---|---|---|---|---|---|
| | | | Mean | Std | Min | Max |
| ABD | Male | 370 | 40.1 | 10.1 | 19 | 66 |
| PED | Female | 117 | 11.4 | 2.2 | 7 | 15 |
| | Male | 114 | 11.8 | 2.3 | 7 | 15 |
| QBB | Female | 511 | 40.4 | 12.9 | 19 | 81 |
| | Male | 287 | 41.0 | 12.9 | 19 | 81 |

QBB, Qatar Biobank cohort; ABD, adult blood bank donors; PED, pediatric subjects.

**Supplemental Table 5. Seroprevalence of endemic HCoVs stratified by gender and age group**

| Species | Age group | Gender | Prevalence (%) | Mean prevalence per age group (%) |
|---|---|---|---|---|
| HCoV-229E | adults | female | 4.3 | 11.7 |
| | | male | 19.0 | |
| | children | female | 10.3 | 8.2 |
| | | male | 6.1 | |
| HCoV-HKU1 | adults | female | 4.1 | 6.5 |
| | | male | 8.8 | |
| | children | female | 7.7 | 6.5 |
| | | male | 5.3 | |
| HCoV-NL63 | adults | female | 9.2 | 13.0 |
| | | male | 16.7 | |
| | children | female | 21.4 | 23.8 |
| | | male | 26.3 | |
| HCoV-OC43 | adults | female | 4.1 | 5.8 |
| | | male | 7.5 | |
| | children | female | 14.5 | 12.5 |
| | | male | 10.5 | |

The adult group (*n* = 1168) includes adult blood bank donors and individuals of the Qatar Biobank cohort.

**Supplemental Table 6. List of peptides that were differentially enriched in children (*n* = 231) versus adults (*n* = 1168)**

| UniProtKB entry | Start[A] | End[A] | Protein symbol | Species | lod | $Log_{10}$ *P* value | Cluster no. | Cluster annotation[B] / peptide location |
|---|---|---|---|---|---|---|---|---|
| P0C6X6 | 1401 | 1456 | pp1ab | HCoV-OC43 | 6.4 | 4.7 | 136 | Papain-like proteinase |
| Q0ZJJ1 | 813 | 868 | pp1ab | HCoV-HKU1 | 6.3 | 3.9 | 102 | Papain-like proteinase |
| Q0ZJJ1 | 225 | 280 | pp1ab | HCoV-HKU1 | 6.0 | 3.1 | 38 | 3C-like proteinase |
| P0C6X2 | 7029 | 7084 | pp1ab | HCoV-HKU1 | 6.0 | 3.1 | 117 | 2'-O-methyltransferase |
| Q5MQD0 | 365 | 420 | S | HCoV-HKU1 | 6.0 | 3.1 | 189 | S1 chain region |
| Q0ZJJ1 | 5825 | 5880 | pp1ab | HCoV-HKU1 | 5.7 | 2.4 | 9 | RNA virus helicase |
| P0C6X5 | 3753 | 3808 | pp1ab | HCoV-NL63 | 5.7 | 2.4 | 10 | Non-structural protein 8 |
| Q0QJI4 | 337 | 392 | S | HCoV-OC43 | 5.7 | 2.4 | 98 | S1/S2 cleavage site |
| **P0C6X3** | **5489** | **5544** | **pp1ab** | **HCoV-HKU1** | **4.5** | **12.3** | **8** | **Helicase** |
| Q6Q1R9 | 197 | 226 | M | HCoV-NL63 | 3.2 | 3.2 | 185 | Interaction with N protein region |
| P0C6X6 | 2381 | 2436 | pp1ab | HCoV-OC43 | 3.2 | 3.2 | 253 | Non-structural protein 3 |
| Q6Q1S2 | 421 | 476 | S | HCoV-NL63 | 3.0 | 2.5 | 131 | S1 chain region |
| Q6Q1S2 | 449 | 504 | S | HCoV-NL63 | 3.0 | 2.5 | 131 | S1 chain region |
| P0C6X1 | 1373 | 1428 | pp1ab | HCoV-229E | 3.0 | 2.5 | 235 | Non-Structural protein 3 |
| P0C6X2 | 3305 | 3360 | pp1ab | HCoV-HKU1 | 2.7 | 5.0 | 13 | Region of 3C-like proteinase |
| **Q6Q1R8** | **29** | **84** | **N** | **HCoV-NL63** | **2.5** | **6.0** | **49** | **N-terminal RNA binding domain** |
| **E2DNV6** | **1** | **56** | **N** | **HCoV-NL63** | **2.2** | **7.3** | **37** | **N-terminal RNA binding domain** |
| Q6Q1R8 | 169 | 224 | N | HCoV-NL63 | 1.8 | 2.4 | 37 | N-terminal RNA binding domain |
| Q5SBN5 | 1 | 56 | N | HCoV-NL63 | 1.8 | 2.4 | 49 | N-terminal RNA binding domain |
| **Q6Q1R8** | **197** | **252** | **N** | **HCoV-NL63** | **1.8** | **7.8** | **37** | **N-terminal RNA binding domain** |
| **Q5MQC5** | **1** | **56** | **ORF8** | **HCoV-HKU1** | **1.7** | **5.9** | **41** | **N-terminal RNA binding domain** |
| **Q6Q1R8** | **337** | **377** | **N** | **HCoV-NL63** | **1.6** | **24.6** | **132** | **C-terminal of dimerization domain** |
| **P0C6X2** | **5461** | **5516** | **pp1ab** | **HCoV-HKU1** | **1.5** | **2.8** | **34** | **RNA virus helicase C-terminal** |
| **P0C6X5** | **4285** | **4340** | **pp1ab** | **HCoV-NL63** | **1.5** | **2.5** | **78** | **RNA-directed RNA polymerase** |
| **E2DNV6** | **29** | **84** | **N** | **HCoV-NL63** | **1.5** | **8.5** | **37** | **N-terminal RNA binding domain** |
| **Q5SBN5** | **29** | **83** | **N** | **HCoV-NL63** | **1.5** | **3.2** | **49** | **N-terminal RNA binding domain** |
| **Q0ZJJ1** | **1121** | **1176** | **pp1ab** | **HCoV-HKU1** | **1.4** | **4.6** | **12** | **Asp-rich region, Papain-like proteinase** |
| **P15423** | **645** | **700** | **S** | **HCoV-229E** | **1.3** | **2.8** | **16** | **Furin-like S2' cleavage site** |
| **G9G2X4** | **1** | **56** | **N** | **HCoV-HKU1** | **1.2** | **5.3** | **41** | **N-terminal RNA binding domain** |
| **Q01455** | **197** | **230** | **M** | **HCoV-OC43** | **1.2** | **3.5** | **147** | **Interaction with N protein region** |
| **Q6Q1R8** | **309** | **364** | **N** | **HCoV-NL63** | **1.1** | **9.5** | **132** | **C-terminus of dimerization domain** |
| **P0C6X2** | **4509** | **4564** | **pp1ab** | **HCoV-HKU1** | **1.1** | **3.6** | **2** | **RNA-directed RNA polymerase** |
| **Q0QJI4** | **757** | **812** | **S** | **HCoV-OC43** | **1.0** | **4.9** | **46** | **Receptor binding domain** |
| **Q5MQC5** | **29** | **84** | **ORF8** | **HCoV-HKU1** | **1.0** | **3.0** | **41** | **N-terminal RNA-binding domain** |
| **P0C6X2** | **1065** | **1120** | **pp1ab** | **HCoV-HKU1** | **0.9** | **2.8** | **12** | **Asp-rich region, Papain-like proteinase** |
| **P0C6X1** | **5377** | **5432** | **pp1ab** | **HCoV-229E** | **-2.2** | **2.4** | **9** | **RNA virus helicase** |
| **Q0ZJJ1** | **965** | **1020** | **pp1ab** | **HCoV-HKU1** | **-2.7** | **26.8** | **12** | **Asp-rich region, Papain-like proteinase** |
| **P0C6X4** | **897** | **952** | **pp1ab** | **HCoV-HKU1** | **-3.0** | **6.5** | **12** | **Asp-rich region, Papain-like proteinase** |
| **Q0ZJG7** | **925** | **980** | **pp1ab** | **HCoV-HKU1** | **-3.4** | **40.7** | **12** | **Asp-rich region, Papain-like proteinase** |
| **P0C6X4** | **925** | **980** | **pp1ab** | **HCoV-HKU1** | **-3.6** | **65.2** | **12** | **Asp-rich region, Papain-like proteinase** |
| **P0C6X3** | **925** | **980** | **pp1ab** | **HCoV-HKU1** | **-3.6** | **65.4** | **12** | **Asp-rich region, Papain-like proteinase** |
| **P0C6X4** | **953** | **1008** | **pp1ab** | **HCoV-HKU1** | **-4.0** | **81.9** | **12** | **Asp-rich region, Papain-like proteinase** |
| **P0C6X2** | **1037** | **1092** | **pp1ab** | **HCoV-HKU1** | **-4.0** | **66.6** | **12** | **Asp-rich region, Papain-like proteinase** |
| **P0C6X4** | **1009** | **1064** | **pp1ab** | **HCoV-HKU1** | **-4.1** | **89.8** | **12** | **Asp-rich region, Papain-like proteinase** |
| **Q0ZJJ1** | **1037** | **1092** | **pp1ab** | **HCoV-HKU1** | **-4.2** | **106.1** | **12** | **Asp-rich region, Papain-like proteinase** |
| **P0C6X3** | **1009** | **1064** | **pp1ab** | **HCoV-HKU1** | **-4.3** | **94.1** | **12** | **Asp-rich region, Papain-like proteinase** |
| **P0C6X2** | **951** | **1006** | **pp1ab** | **HCoV-HKU1** | **-4.3** | **114.6** | **12** | **Asp-rich region, Papain-like proteinase** |
| **P0C6X3** | **1037** | **1092** | **pp1ab** | **HCoV-HKU1** | **-4.4** | **105.0** | **12** | **Asp-rich region, Papain-like proteinase** |
| **P0C6X4** | **981** | **1036** | **pp1ab** | **HCoV-HKU1** | **-4.9** | **139.5** | **12** | **Asp-rich region, Papain-like proteinase** |
| **P0C6X2** | **925** | **980** | **pp1ab** | **HCoV-HKU1** | **-5.2** | **147.1** | **12** | **Asp-rich region, Papain-like proteinase** |
| **Q0ZJJ1** | **925** | **980** | **pp1ab** | **HCoV-HKU1** | **-5.3** | **153.3** | **12** | **Asp-rich region, Papain-like proteinase** |
| **P0C6X3** | **953** | **1008** | **pp1ab** | **HCoV-HKU1** | **-5.5** | **162.7** | **12** | **Asp-rich region, Papain-like proteinase** |
| **P0C6X3** | **951** | **1006** | **pp1ab** | **HCoV-HKU1** | **-5.9** | **183.5** | **12** | **Asp-rich region, Papain-like proteinase** |
| **Q0ZJJ1** | **1093** | **1148** | **pp1ab** | **HCoV-HKU1** | **-6.0** | **182.1** | **12** | **Asp-rich region, Papain-like proteinase** |
| **P0C6X2** | **949** | **1004** | **pp1ab** | **HCoV-HKU1** | **-6.2** | **192.8** | **12** | **Asp-rich region, Papain-like proteinase** |
| **Q0ZJJ1** | **953** | **1008** | **pp1ab** | **HCoV-HKU1** | **-6.2** | **190.9** | **12** | **Asp-rich region, Papain-like proteinase** |
| **P0C6X2** | **953** | **1008** | **pp1ab** | **HCoV-HKU1** | **-6.2** | **195.5** | **12** | **Asp-rich region, Papain-like proteinase** |
| **Q0ZJJ1** | **979** | **1034** | **pp1ab** | **HCoV-HKU1** | **-6.6** | **204.6** | **12** | **Asp-rich region, Papain-like proteinase** |
| **P0C6X4** | **4761** | **4816** | **pp1ab** | **HCoV-HKU1** | **-7.1** | **21.0** | **36** | **RNA-directed RNA polymerase** |
| **Q0ZJG7** | **4985** | **5040** | **pp1ab** | **HCoV-HKU1** | **-8.1** | **47.6** | **21** | **3C-like proteinase** |
| **P0C6X1** | **337** | **392** | **pp1ab** | **HCoV-229E** | **-9.8** | **128.6** | **219** | **Non-structural protein 2** |

[A]Start and end position of enriched peptides relative to the amino acid sequences in UniProtKB. [B]Cluster annotation was adapted from UniProtKB entry descriptions and features. Only peptides with a log odds ratio (lod) ≥ ln(2) or ≤ ln(-2) and a *P* value < 0.005 (Fisher's exact test) are listed. Immunodominant peptides (i.e., peptides found to be significantly enriched in ≥1% of samples of the tested individuals (*N* = 1399)) are marked in bold font.

**Supplemental Table 7. Demographic data and sample collection for COVID-19 patients**

| Patient no. | Age | Gender | Nationality | Time from onset of symptoms to sample collection |
|---|---|---|---|---|
| **1** | 49 years | Female | Belgian | 25 days, 55 days |
| **2** | 68 years | Male | Pakistani | 5 days |
| **3** | 30 years | Male | Egyptian | 12 days |
| **4** | 49 years | Male | Indian | 10 days |
| **5** | 68 years | Male | Sudanese | 9 days |
| **6** | 56 years | Male | Indian | 10 days |
| **7** | 67 years | Male | Indian | 12 days |

**Supplemental Table 8. Peptides enriched by PhIP-Seq in COVID-19 patients (*n* = 7)**

| UniProtKB entry | Start[A] | End[A] | Species | Protein symbol | Cluster no. | No. of samples enriched | Cluster annotation[B] / peptide location |
|---|---|---|---|---|---|---|---|
| **K9N5Q8** | 841 | 896 | MERS-CoV | S | 16 | 2 | Furin-like S2' cleavage site |
| **Q91A26** | 869 | 924 | Beta-CoV-1[C] | S | 16 | 2 | Furin-like S2' cleavage site |
| **Q5MQD0** | 897 | 952 | HCoV-HKU1 | S | 19 | 3 | Furin-like S2' cleavage site |
| **Q14EB0** | 897 | 952 | HCoV-HKU2 | S | 19 | 3 | Furin-like S2' cleavage site |
| **Q14EB0** | 869 | 924 | HCoV-HKU3 | S | 19 | 2 | Furin-like S2' cleavage site |
| **A0A0U2V9P1** | 85 | 140 | MERS-CoV | S | 19 | 2 | Furin-like S2' cleavage site |
| **A0A023Y9K3** | 813 | 868 | MERS-CoV | S | 19 | 3 | Furin-like S2' cleavage site |
| **A0A023Y9K3** | 841 | 896 | MERS-CoV | S | 19 | 3 | Furin-like S2' cleavage site |
| **T2BBI8** | 869 | 924 | MERS-CoV | S | 19 | 3 | Furin-like S2' cleavage site |
| **P59594** | 785 | 840 | SARS-CoV | S | 19 | 6 | Furin-like S2' cleavage site |
| **Q91A26** | 897 | 952 | Beta-CoV-1[C] | S | 19 | 4 | Furin-like S2' cleavage site |
| **U5NJG5** | 1177 | 1232 | MERS-CoV | S | 59 | 3 | Heptad repeat 2 |
| **U5NJG5** | 1205 | 1260 | MERS-CoV | S | 59 | 3 | Heptad repeat 2 |
| **K9N5Q8** | 1205 | 1260 | MERS-CoV | S | 59 | 2 | Heptad repeat 2 |
| **K9N5Q8** | 337 | 392 | MERS-CoV | S | 71 | 2 | Receptor binding region |
| **P59594** | 1093 | 1148 | SARS-CoV | S | 91 | 4 | Heptad repeat 2 |
| **P59594** | 1121 | 1176 | SARS-CoV | S | 91 | 6 | Heptad repeat 2 |
| **Q14EB0** | 1149 | 1204 | HCoV_HKU1 | S | 140 | 2 | Upstream of heptad repeat 2 |
| **Q91A26** | 1205 | 1260 | Beta-CoV-1[C] | S | 181 | 3 | Heptad repeat 2 |
| **P59594** | 533 | 588 | SARS-CoV | S | 245 | 2 | C-terminal of receptor binding domain |
| **Q8BB23** | 197 | 252 | Beta-CoV-1[C] | N | 15 | 2 | SR-rich region |
| **P59595** | 141 | 196 | SARS-CoV | N | 25 | 4 | N-terminal RNA-binding domain |
| **P59595** | 197 | 252 | SARS-CoV | N | 25 | 5 | SR-rich region |
| **Q6Q1R8** | 337 | 377 | HCoV-NL63 | N | 132 | 2 | C terminus |
| **P59595** | 365 | 420 | SARS-CoV | N | 243 | 4 | C terminus |
| **A0A075Q443** | 169 | 224 | MERS-CoV | pp1a | 24 | 2 | NA |
| **W6A0R5** | 1121 | 1176 | MERS-CoV | pp1a | 57 | 2 | Papain-like proteinase |
| **K9N7C7** | 5489 | 5544 | MERS-CoV | pp1ab | 8 | 4 | Helicase |
| **Q0ZJJ1** | 953 | 1008 | HCoV-HKU1 | pp1ab | 12 | 2 | Asp-rich region, Papain-like proteinase |
| **P0C6X2** | 953 | 1008 | HCoV-HKU1 | pp1ab | 12 | 4 | Asp-rich region, Papain-like proteinase |
| **P0C6X2** | 949 | 1004 | HCoV-HKU1 | pp1ab | 12 | 5 | Asp-rich region, Papain-like proteinase |
| **P0C6X3** | 951 | 1006 | HCoV-HKU1 | pp1ab | 12 | 3 | Asp-rich region, Papain-like proteinase |

[A]Start and end position of enriched peptides relative to the amino acid sequences in UniProtKB. [B]Cluster annotation was adapted from UniProtKB entry descriptions and features. [C]Non-human CoV isolate. Only peptides that were significantly enriched in two or more patients are listed.